A Multiobjective Design Optimization Procedure for Control of Structures Using Piezoelectric Materials

Aditi Chattopadhyay and Charles E. Seeley

Journal of Intelligent Material Systems and Structures 1994 5: 403
DOI: 10.1177/1045389X9400500313

A Multiobjective Design Optimization Procedure for Control of Structures Using Piezoelectric Materials

ADITI CHATTOPADHYAY* AND CHARLES E. SEELEY
Department of Mechanical and Aerospace Engineering
Arizona State University
Tempe, AZ 85287

ABSTRACT: Piezoelectric materials can be used as sensors and actuators for structures that require active vibration control and lack sufficient stiffness or passive damping. Efficient implementation of these actuators requires that their optimal locations on the structure be determined and that the structure be designed to best utilize the properties of the actuators. A formal optimization procedure has been developed to address both of these issues. A gradient based multiobjective optimization technique is used to minimize multiple and conflicting design objectives associated with both the structure and the control system design which is also coupled with the actuator location problem. Objective functions such as the fundamental natural frequency of the structure and energy dissipated by the piezoelectric actuators are included in this study. Constraints are placed on the mass of the structure, displacements and applied voltage to the piezoelectric actuators. Design variables include parameters defining both the control system and the structure. The finite element method is used to model active damping elements which are piezoelectric actuators bonded to a box beam. The optimization procedure is implemented on a flexible 2-D frame.

INTRODUCTION

VIBRATION in structures is an important issue in engineering design. Both active and passive vibration damping techniques have been explored. Previously, heavy stiffening members and non-structural masses have been used to address the issue of reducing oscillatory motion, which incorporates a weight penalty. Active vibration suppression techniques offer definite advantages compared to conventional methods and are currently being pursued. Such techniques can result in increased performance and service life of the structure while reducing the total weight. Recently, the use of smart materials for active vibration control has been studied by many researchers (Banks et al., 1993; Banks et al., 1992; Dosch et al., 1992; Hanagud et al., 1992; Gibbs et al., 1991; Heeg, 1991; Sepulveda et al., 1992; Dimitriadis et al., 1989). Piezoelectric materials are currently available that produce an electric field in response to a mechanical deformation. Conversely, a significant deformation is observed in the plane of the material when a voltage is applied across the thickness. When placed in discrete locations on a structure, piezoelectrics can sense movement in a structure and control that motion via localized strains. Thus, piezoelectric materials can act as both sensors and actuators in the role of active vibration dampers for structures.

It is desirable to determine the best locations for piezoelectric actuators on a structure in order to achieve the most efficient implementation of their special properties, as well as for economic feasibility. In most of the earlier work in this area, trial and error techniques have been used and parametric studies have been performed (Heeg, 1991). Recently, there has been some interest in using formal optimization strategies for optimal placement of the actuators. Horner (1985) developed a continuous optimization procedure using actuator gains as a basis for elimination of non-optimal actuator locations. This method has two drawbacks. First, a design variable for each actuator location is computationally expensive for large systems due to the gradient information required during optimization. Second, the magnitude of each gain does not necessarily correspond to the energy dissipated by each actuator. Therefore, elimination of actuators with small gains does not necessarily improve the performance of the structure and control system interaction. Integer optimization techniques such as genetic algorithms and simulated annealing have also been used to determine optimal actuator locations (Onoda et al., 1992). Although these methods are often successful in determining more efficient actuator locations, they do not address the influence of structural parameters which are continuous variables and, when included, can enhance the performance of the piezoelectric control system. For instance, a small change in the cross-sectional area of the structural members can have a significant influence on the work required by the actuators to control the structure. An increase in cross section results in increased stiffness, which reduces the work required by the actuators to control the structure. However,

Associate Editor: Dr. H. T. Banks.
*Author to whom correspondence should be addressed.

1045-389X/94/03 0403-09 $6.00/0

this also introduces a weight penalty and affects the efficiency of the actuators. The influence of structural parameters on the control system has not been addressed extensively in the literature. Sepulveda et al. (1992) approximated the discrete optimization problem with a continuous problem in order to include continuous design variables in the formulation. To efficiently address the design of the structure and the control system, it is also necessary to include design criteria pertaining to each of these disciplines. For example, to efficiently control vibration, it is necessary to minimize the energy dissipated by the actuators as well as to maximize the fundamental natural frequency of the structure in order to avoid possible resonance with the disturbance force. This leads to a multiple objective design optimization problem.

In this paper, a formal optimization procedure has been developed using a continuous approach. The procedure addresses multiple design objectives. The objective is to minimize the energy dissipated by the actuators to control the structure without incorporating a weight penalty. The fundamental natural frequency is also maximized as an objective function. This is coupled with the problem of finding the optimal placement and the number of actuators necessary for controlling vibration. Design variables include the magnitude of the actuator gains and cross-sectional areas of the structural members. A multiobjective design optimization technique is used (Chattopadhyay et al., 1991), and the optimization is performed using a code that is based on the method of feasible directions (Vanderplaats, 1973).

PROBLEM DESCRIPTION

A formal optimization procedure is developed to address the efficient implementation of piezoelectric actuators for vibration control. Both the placement of the fixed length actuators and the design of the structure are coupled within the optimization problem. The procedure developed is applied to a 2-D flexible structure subjected to a dynamic loading, which is controlled by a distributed system of piezoelectric actuators. Box beam elements are developed for use as structural elements in the finite element discretization of the frame structure to be examined.

FORMULATION

In this study, peizoelectric actuators are assumed to be surface bonded to a box beam with a strong adhesive such as epoxy. It is assumed that for a thin bonding layer, the effects of bonding on the efficiency of the actuators is negligible (Crawley and de Luis, 1987). The piezoceramic PZT G-1195 is the piezoelectric material used for the actuators due to its high stress and low strain characteristics when compared to other piezoelectric materials such as polymer piezoelectrics (Piezo Systems Inc., 1993). Box beam elements, which are used in this study to model the beam cross section, are efficient structural components used in many aerospace applications. It is assumed that sensors and actuators are collocated to avoid problems with stability. Figure 1 shows actuators, which are poled in the thickness direction, that are bonded at the same location on both the top and bottom surfaces of a flat plate. If the applied voltage to each actuator has the same polarity as in Figure 1(a), extension along the x axis will result since both actuators will act in the same direction. Similarly, if the polarity is reversed for one of the actuators, as shown in Figure 1(b), one actuator will act in tension and the other in compression. This results in an effective bending moment applied to the plate at the location of the actuators. Examining Figure 1(a), in which both actuators act in the same direction, the strain distribution across the plate is assumed to be constant. The force, F, resulting from this configuration is given as follows (Crawley and de Luis, 1987):

$$F = \frac{E_B t_B b}{2 + \psi} [\epsilon_B - \Lambda] \tag{1}$$

where E_B is the elastic modulus of the substructure, t_B is the thickness of the substructure, and ϵ_B is the strain in the substructure. The width of the box beam, b, and the width of the actuator are assumed to be equal. The quantity ψ is a dimensionless ratio relating the stiffness of the piezoceramic actuators to the stiffness of the substructure, and Λ is the strain in the plane of the actuator resulting from an applied electric field to the piezoceramic actuator. These quantities are defined below:

$$\psi = \frac{E_B t_B}{E_C t_C} \tag{2}$$

$$\Lambda = \frac{d_{31} V}{t_C} \tag{3}$$

where the quantity t_C is the thickness of the piezoceramic actuator, d_{31} is the piezoelectric strain constant and V is the applied voltage in the appropriate direction.

Figure 2 shows a box beam with uniform wall thickness (t_B). If t_B and the thickness of the piezoelectric actuators, t_C,

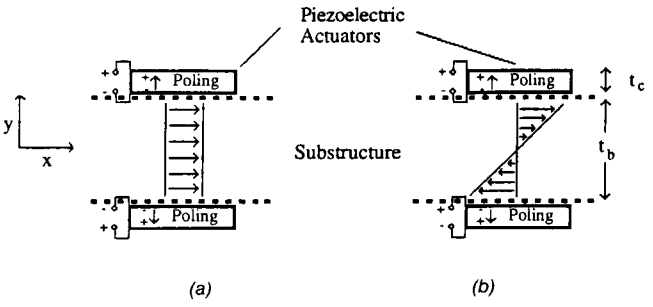

Figure 1. *Strain distribution resulting from piezoelectric actuators: (a) same polarity top and bottom and (b) opposite polarity.*

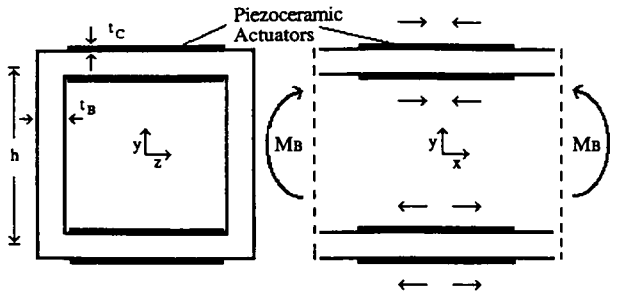

Figure 2. *Placement of piezoelectric actuators on a box beam.*

are significantly smaller than the height, h, of the beam, the strain distribution in the top and bottom webs of the box beam and the piezoelectric actuators is approximately constant for an applied bending moment, although opposite in sign. It is therefore desirable to have both of the top web actuators act in the same direction. Similarly, it is desirable to have both the actuators on the lower web act in a direction opposite to that of the actuators on the upper web. This results in an effective bending moment M_B given by:

$$M_B = F\,h \tag{4}$$

where F is the force developed in the actuators from Equation (1). From beam theory, the strain ϵ_B at any point along the beam is given as follows:

$$\epsilon_B = -\frac{d\phi}{dx}\,y \tag{5}$$

where ϕ is the rotation. The voltage V_i applied to the ith piezoelectric actuator, which is the rate feedback related quantity, is represented as follows:

$$V_i = G_i\dot{\phi}_i \tag{6}$$

where G_i is the gain, $\dot{\phi}_i$ is the angular velocity of the beam, and the dot indicates a derivative with respect to time. Assuming a square cross section so that $b = h$, the bending moment, M_B, on the box beam can be expressed as follows:

$$M_B = -\frac{E_B t_B h^2}{2+\psi}\left[\frac{h}{2}\frac{d\phi}{dx}\right] - \frac{E_B t_B h^2}{2+\psi}\left[\frac{d_{31}G_i\dot{\phi}_i}{t_C}\right] \tag{7}$$

In Equation (7), the first term represents the passive stiffness of the actuators and the second term represents the active control properties. Using a finite elements approach, the passive stiffness properties of the piezoelectric actuators from the first term of Equation (7) are added to the normal beam element stiffness matrix, creating an augmented stiffness matrix $\underset{\sim}{K}^*$ as shown in Equation (8a) (Hanagud et al., 1992). It must be noted that the passive stiffness properties of the actuators in the augmented stiffness matrix are included only where actuator locations exist. Similarly, an augmented mass matrix $\underset{\sim}{M}^*$ is created which includes the mass of the structure and the mass of the actuators where they exist on the structure [Equation (8b)]. The augmented stiffness and mass matrices are represented as follows:

$$\underset{\sim}{K}^* = \underset{\sim}{K}_B + \underset{\sim}{K}_C \tag{8a}$$

$$\underset{\sim}{M}^* = \underset{\sim}{M}_B + \underset{\sim}{M}_C \tag{8b}$$

where the subscript B corresponds to the beam elements and the subscript C corresponds to the piezoelectric actuators. The global second order equations of motion, with n degrees of freedom and without damping and forcing function, are written as:

$$\underset{\sim}{M}^*\ddot{\bar{q}} + \underset{\sim}{K}^*\bar{q} = \bar{0} \tag{9}$$

where

$\bar{q} = \begin{bmatrix} x \\ y \\ \phi \end{bmatrix}$. The $2n$ state space control law is written as:

$$\frac{d}{dt}\begin{bmatrix}\bar{q}\\ \dot{\bar{q}}\end{bmatrix} = \underset{\sim}{A}\begin{bmatrix}\bar{q}\\ \dot{\bar{q}}\end{bmatrix} + \underset{\sim}{B}[\bar{u}] \tag{10}$$

where

$$\underset{\sim}{A} = \begin{bmatrix} \underset{\sim}{0} & \underset{\sim}{I} \\ -\underset{\sim}{M}^{*-1}\underset{\sim}{K}^* & \underset{\sim}{0} \end{bmatrix} \tag{11}$$

$$\underset{\sim}{B} = \begin{bmatrix} \underset{\sim}{0} \\ -\underset{\sim}{M}^{*-1}\underset{\sim}{C} \end{bmatrix} \tag{12}$$

The identity matrix is denoted $\underset{\sim}{I}$, and $\underset{\sim}{C}$ is the gain matrix obtained from the second term of Equation (7). The inplane force developed by the piezoceramic actuators [Equation (1)] occurs at the endpoints of the actuators. Since the actuators cover the entire length of the box beam elements, the effect of the actuators is the application of an external bending moment at the nodes of each active element. Negative velocity feedback (rate feedback) is used in conjunction with the gain matrix to represent this applied bending moment. Since $[\bar{u}] = [\dot{\bar{q}}]$, the control gain matrix acts in a manner analogous to that of a structural damping matrix. Therefore, the actuators assume the role of active damper elements. The motivation of the present work is to study the active damping effects of the piezoceramic actuators. Therefore, only the active damping of the control system is retained in the analysis and any passive structural damping is ignored.

A disturbance is applied to the uncontrolled structure over a time interval $0 \le t \le t_a$. The actuators become active during a time period $t_a \le t \le t_b$ in order to damp out the

vibrations caused by the disturbance from the previous time period. Finally, the undamped system is checked during the time interval $t_b \leq t \leq t_c$ to ensure that the total energy of the system has been reduced to a specified level. It is unrealistic to expect the energy of the system to be reduced to zero at $t = t_c$. Normally, mission requirements specify the energy to be reduced to some fraction of the initial energy (Horner and Walz, 1985).

Eigenvalues and eigenvectors of the second order undamped system from Equation (9) are determined so that modal summation techniques can be applied. Four modes are retained in this analysis. The active damping matrix is not proportional to the mass and stiffness matrices, so techniques that take advantage of that situation are not applicable. As a result, the equations do not decouple. However, a reduced modal space is used for solving the equations of motion using a numerical ordinary differential equation integration technique. It is computationally efficient and significantly reduces CPU time. It also eliminates problems related to controlling higher modes which do not have significant contributions to the overall motion.

OPTIMIZATION PROBLEM

An optimization procedure has been developed in which the choice of optimal actuator locations is made on the basis of the energy dissipated by the actuator at each location. Multiple objective functions are combined into a single objective to be minimized by the optimizer. Actuator locations that have small contributions to the overall reduction of the energy in the system are eliminated. Only actuator locations with significant contributions to the dissipated energy are retained. In the algorithm developed here, all the actuators are assumed to have the same gain. Therefore, a single design variable for the gain of all actuators is used. This significantly reduces computational cost. Fixed length actuators are initially placed in all possible locations on the structure, which are the discretized elements. Next, the total energy dissipated by the actuators required to control the structure is minimized using a gradient based optimization procedure. The energy dissipated by each actuator is determined and actuator locations which dissipate significantly less energy, compared to the rest of the actuators, are eliminated as possible locations, a few at a time, by setting their gains to zero and removing their properties from the augmented stiffness and mass matrices. This involves restarting the optimization procedure several times once convergence is obtained for each actuator configuration. Actuator dimensions do not change during optimization. The optimal configuration is reached when the removal of additional actuators leads to violation of one or more of the constraints. Convergence is based on a relative change of less than 0.5% of the objective function values for three consecutive optimization cycles once all constraints are satisfied. In the following sections, further details of the optimization problem formulation are presented.

Objective Functions

The first objective is to determine the optimal locations of the piezoelectric actuators by minimizing the total dissipated energy. The energy dissipated by each actuator can be expressed as the integral over the time period of active control ($t_a \leq t \leq t_b$) for each actuator. The total energy, J, to be minimized is the sum of these integrals and is given as follows (Horner and Walz, 1985).

$$J = \sum_{i=1}^{IACT} \int_{t_a}^{t_b} \dot{q}_i^T \underset{\sim}{c}_i \dot{q}_i dt \tag{13}$$

where $IACT$ is the current number of elements that are considered as possible actuator locations, and $\underset{\sim}{c}_i$ is the individual gain matrix of the ith active damping element. The second objective is to maximize the fundamental frequency, ω_1, of the structure to avoid possible resonance with the forcing frequency and thereby reduce vibration. These design objectives are combined into a single objective function F using a multiobjective formulation technique described later.

Constraints

It is desired that the total energy, E, of the structure, which is the sum of the potential and the kinetic energies, is reduced to a specified fraction of the original energy after the time interval $T = t_b - t_a$. Therefore, a constraint is imposed as follows:

$$E_{fin} \leq \gamma E_{int} \tag{14}$$

where γ is the desired fraction of the initial energy remaining in the system after the specified time T and the subscripts "int" and "fin" refer to the initial and the final states, respectively.

Also, a piezoelectric material is associated with a maximum electric field E_{max}. Exceeding this value can result in the loss of the material's special properties. Correspondingly, there exists a maximum voltage V_{max} that can be applied to a piezoelectric actuator which must not be exceeded. The voltage is checked at each time step of the design optimization procedure. Noting that $V_i = G_i \dot{\phi}_i$ for each actuator [Equation (6)], when $V_i \geq V_{max}$, saturation occurs and the gain for the next time step for that actuator is set to:

$$G_i = \frac{V_{max}}{\dot{\phi}_i} \tag{15}$$

This ensures that $V_i \leq V_{max}$ without introducing any new design variables. As the number of actuators is reduced during the optimization process, the voltage to the remaining actuators increases in order to redistribute the control forces necessary for satisfying all of the constraints.

The desired modal damping ratio ζ_i, corresponding to the jth mode, can be expressed as:

$$\zeta_j = \frac{\ln(1/\epsilon)}{\omega_j T} \tag{16}$$

where ω_j is the jth undamped natural frequency of the structure and ϵ is the fraction of the initial vibration amplitude which remains in the structure after the time interval T. The damped eigenvalues occur in complex conjugate pairs from Equation (10) and assume the following form:

$$\lambda_j = a \pm \mathbf{i}b \tag{17}$$

where $\mathbf{i} = \sqrt{-1}$, the real part $a = -\bar{\zeta}_j\omega_j$, the imaginary part $b = \omega_j\sqrt{1 - \bar{\zeta}_j^2}$, and $\bar{\zeta}_j$ are the actual damping ratios. To ensure stability of the structural system, it is assumed that sensors and actuators are collocated. Most of the energy in the system is assumed to be located in the lower modes, which are included in the displacement constraints to ensure stability. Any noise in the control system is assumed to be negligible. In addition, the following constraint is imposed on the real part of the complex eigenvalues:

$$a \leq 0 \tag{18}$$

Solving for $\bar{\zeta}_j$ from Equation (17), the following constraint is imposed to ensure that the desired damping ratios are achieved.

$$\bar{\zeta}_j \geq \zeta_j \tag{19}$$

It must be noted that the gain matrix $\underset{\sim}{C}$ is not constant since it is altered at each time step to ensure that the voltage does not exceed V_{max}. Therefore, $\bar{\zeta}_j$ is not constant over time. A minimum gain matrix is obtained at maximum velocity when saturation occurs. The maximum gain matrix is found when V_{max} is not exceeded by any one of the actuators. In order to evaluate the damping ratio constraint, constant damping ratios are determined by using a gain matrix which is averaged over the time interval when the actuators are active. Although these averaged damping ratios cannot be used to construct an analytical solution of the decaying motion, they approximately describe the character of the solution to ensure that proper damping does occur in the desired modes. The weighted average will fit between the minimum and the maximum damping factors calculated from the minimum and the maximum gains, respectively, as seen in Figure 3.

Since the mass of the structure can increase through an increase in box beam thickness in order to stiffen the structure and minimize the energy dissipated by the actuators, it is important to impose a constraint on the total mass of the structure:

$$m \leq \bar{m} \tag{20}$$

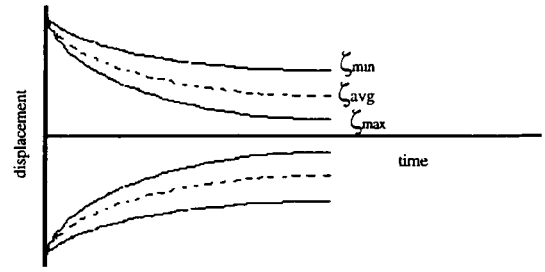

Figure 3. *Character of solution with variation in damping factors.*

where m is the mass of the structure and $\bar{m}$ is the allowable mass.

Design Variables

A single positive gain, representing all actuators, is used as a design variable along with web thicknesses of each box beam element. It is assumed that the height of each beam element, h, is equal and not varied during optimization. This allows the moment arm for the actuators to be the same for all elements for consistent results.

Multiobjective Optimization Formulation

To efficiently formulate the above optimization problem associated with multiple design objectives such as energy dissipated by the actuators, J, and the fundamental natural frequency, ω_1, of the structure, a multiobjective formulation technique known as the Minimum Sum Beta (Min$\Sigma\beta$) approach (Chattopadhyay and McCarthy, 1991) is used. Using this approach, each original objective function is introduced as a new constraint in addition to the original constraints. The new constraints assume the following form:

$$gk = \frac{(f(\Phi)_k - f(\Phi)_k^*)}{f(\Phi)_k^*} \leq \beta_k \quad k = 1, NOBJ \tag{21}$$

where β_k is a new pseudo design variable introduced for each new constraint having properties such that the original objective functions $f(\Phi)_k$ remain within some tolerance of the specified target values denoted $f(\Phi)_k^*$. The design variable vector is Φ and includes the original design variables of the problem along with additional pseudo design variables $\beta_1, \beta_2, \ldots \beta_k$. The quantity $NOBJ$ denotes the total number of original objective functions. The new composite objective function $F(\Phi)$ is formulated as the sum of all the new pseudo design variables and is presented as follows:

$$F(\Phi) = \beta_1 + \beta_2 + \ldots \beta_{NOBJ} = \sum_{K=1}^{NOBJ} \beta_k \tag{22}$$

As the new objective function is minimized, it has the effect of reducing the tolerances between the current and the specified target values of each individual objective function.

The result is the best compromise between all of the original objective functions. The objective function is linear and provides computational advantages.

Implementation

The basic optimization algorithm consists of a nonlinear programming technique for constrained function minimization, based on the method of feasible directions, as implemented in the computer code CONMIN (Vanderplaats, 1973). Since CONMIN requires several objective function and constraint evaluations during its search, the use of an exact analysis for each calculation is computationally prohibitive. Therefore, an approximation technique, known as the two-point exponential approximation (a hybrid technique) developed by Fadel et al. (1990), is used. The two point exponential approximation is an extension of a Taylor series approximation that employs an exponential function which uses function and gradient information from the previous and current design points. The form of this approximation is as follows:

$$\hat{F}(\Phi) = \hat{F}(\Phi_0) + \sum_{n=1}^{NDV} \left(\left(\frac{\varphi_n}{\varphi_{o_n}} \right)^{p_n} - 1.0 \right) \frac{\varphi_{o_n}}{p_n} \frac{\partial F(\Phi_0)}{\partial \varphi_n} \tag{23}$$

where the exponent p_n is given by:

$$p_n = \frac{\log \left(\dfrac{\left(\dfrac{\partial F(\Phi_1)}{\partial \varphi_n} \right)}{\left(\dfrac{\partial F(\Phi_0)}{\partial \varphi_n} \right)} \right)}{\log \left(\dfrac{\varphi_{1_n}}{\varphi_{o_n}} \right)} + 1.0 \tag{24}$$

In the above equation, $\hat{F}(\Phi)$ is the approximated objective function value, the subscripts 0 and 1 refer to the current and previous design points, respectively, and *NDV* denotes the total number of design variables. Similar expressions are derived for the constraints. The exponent p_n is considered to be a "goodness of fit parameter" and varies between 1 and -1. If $p_n = 1$, a linear approximation results, and if $p_n = -1$, a reciprocal approximation results. Values of p_n between 1 and -1 produce a corrected approximation that most appropriately adheres to the current design data. Since p_n lies between 1 and -1, the algorithm for this method is set up such that when $p_n < 1$ it is set equal to 1 and when $p_n > -1$, it is similarly set equal to -1. Care must also be taken to avoid singularities that may occur when using the logarithmic functions. In the event that a singularity arises, the algorithm reverts to a first order linear Taylor series approximation as follows:

$$\hat{F}(\Phi) = \hat{F}(\Phi_0) + \sum_{n=1}^{NDV} (\varphi_n - \varphi_{o_n}) \frac{\partial F(\Phi_0)}{\partial \varphi_n} \tag{25}$$

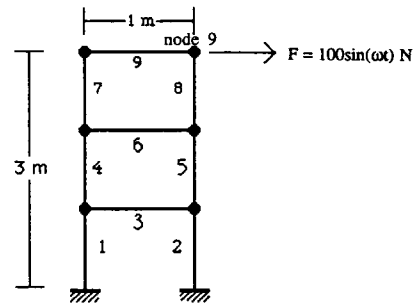

Figure 4. *Finite element discretization of a 2-D frame.*

To reduce possible errors while using either of the above schemes, move limits, defined as the maximum fractional change of a design variable value, are imposed as upper and lower bounds on the design variables, φ_n. Move limits on the order of 5% are imposed to ensure accuracy of the approximation.

RESULTS

A 2-D frame structure with box beam cross section, as shown in Figure 4, is used as the test structure. Piezoceramic actuators are placed on two sides of the box beam elements to create a bending moment about the z axis. It is assumed that the actuators cover the entire length and width of each structural element. The material used is aluminum with a density of 7750 kg/m^3 and an elastic modulus of 68×10^9 N/m^2. PZT G-1195 piezoceramic actuators are used in this analysis and their properties are listed in Table 1. The disturbance is caused by a 100 N sinusodial force with a frequency of 25 Hz applied at node 9 for a period of 0.10 seconds. The constraints imposed are as follows. The energy created by the disturbance force and the displacement magnitudes corresponding to the first four modes must be reduced to 5% of the initial conditions within one second. The structure is discretized using the finite element method. The initial box beam web thickness is 1 mm and h is fixed at 10 cm. Two different optimization problems are solved using the same initial design. A description of the two cases and the corresponding results are described next.

Case 1

In this case, only the energy dissipated by the actuators, J, is minimized using the gain as a single design variable. The optimization is started with a feasible initial design. Actuators are initially placed on each element. The energy dissi-

Table 1. Typical values of PZT G-1195.

E_{max}, V/m	600×10^3
d_{31}, m/V	190×10^{-12}
E_C, N/m^2	63×10^9
t_C, μm	254

pated by each actuator is analyzed. Next, using the optimization procedure developed, actuator locations are eliminated on the basis of the significance of actuator contribution to the overall energy dissipated by the control system. The results of the optimization procedure for case 1 are presented in Table 2. Only a few optimization cycles are necessary for each actuator configuration to converge. Locations where actuators are eliminated, at each iteration, are italicized. Eliminated actuator locations are indicated with a dash (−). The dissipated energy actually increases slightly in iterations 2 and 3, even though it is minimized in the optimization process. This is the result of the optimizer satisfying violated constraints as actuators are eliminated. The final configuration comprises two actuators. Removal of both of these two remaining actuators results in an impractical design since there would then be no actuators left to control the structure. Also, removal of only one of these actuators is not justifiable using the developed algorithm since both actuators dissipate the same amount of energy. The final design contains two actuators located at elements 1 and 2 which are located at the base of the frame structure. Although structural parameters are not altered during optimization, the natural frequency of the structure increases by 18% (26.03 Hz to 30.75 Hz) from initial to final design. This is caused by the removal of 7 actuators which reduces the mass by 5.5 kg, allowing the structure to become more stiff overall. The applied voltage to the actuator at the location of element 1, corresponding to the initial design for both cases, is presented in Figure 5. The maximum allowable voltage, V_{max}, for the piezoelectric material considered here is 152 volts, which is proportional to the material thickness and maximum allowable electric field E_{max}. Saturation occurs at V_{max}. The motion in the structure is initially large enough to cause saturation of the actuators, indicating that ignoring this constraint could result in large voltage spikes which may permanently damage the piezoelectric actuators.

Table 2. Optimization results; Case 1.

		Initial	Iteration 1 (all)	Iteration 2 (−3,6,9)	Iteration 3 (−4,5)	Iteration 4 (−7,8)
Elem. No.						
	1	0.565	0.568	0.624	0.653	0.336
	2	0.565	0.568	0.624	0.653	0.336
Actuator	3	0.000	*0.000*	—	—	—
Energy	4	0.033	0.032	*0.035*	—	—
(Nm)	5	0.033	0.032	*0.035*	—	—
	6	0.000	*0.000*	—	—	—
	7	0.174	0.171	0.191	*0.199*	—
	8	0.174	0.171	0.191	*0.199*	—
	9	0.000	*0.000*	—	—	—
Total energy (Nm)		1.54	1.54	1.70	1.70	0.67
ω_1(Hz)		26.03	26.03	28.83	27.31	30.75
Mass (kg)		10.08	10.08	10.08	10.08	10.08
Gain (*V* sec/*m*) × 10^3		3.00	2.88	2.14	2.00	1.80

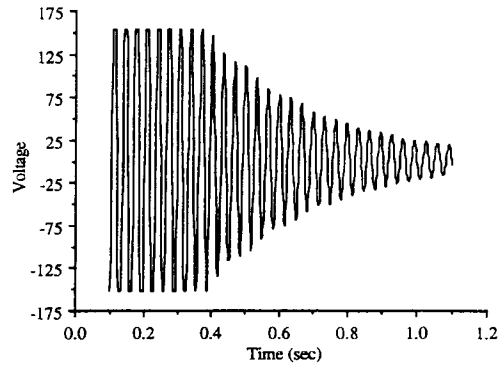

Figure 5. *Applied voltage to actuator 1—initial design.*

Case 2

In this case, the energy dissipated by the actuators is minimized and the first natural frequency of the structure is maximized, simultaneously, using the Min$\Sigma\beta$ multiobjective optimization formulation. The actuator gain and the web thicknesses of the box beam elements are used as design variables. Due to symmetry, the thicknesses of elements 1 and 2 (t_1), 4 and 5 (t_2), 7 and 8 (t_3), and 3, 6 and 9, (t_4) are set to be equal. Lower and upper bounds are imposed on these thicknesses such that 0.5 mm $\geq t_i \geq$ 2.0 mm. The gains of all of the actuators are set to be equal to a single design variable *G*. In addition to the constraints used in Case 1, a constraint is also imposed on the structural mass, i.e. $m \leq \bar{m}$ where $\bar{m}$ = 10.1 kg, which is the initial mass of the structure without the actuators for each initial design. The total weight of the actuators for each structural element is 0.79 kg. The results of the optimization procedure for Case 2 are presented in Table 3. The mass constraint and the displacement constraint corresponding to the first mode remain active throughout the optimization process. The displacement constraint corresponding to the third mode becomes active during the final configuration optimization. The energy constraint is well satisfied throughout the optimization procedure, indicating that stability is maintained in the modes included in this analysis. Figure 6 presents the characteristic decay of the tip displacement amplitude for the structure at node 9 in the final design. It is seen that this displacement constraint is also well satisfied.

Comparison of Cases

Case 2, in which the energy dissipated by the piezoelectric controls and the natural frequency of the structure are used as design objectives, represents a superior design. Figure 7 presents the optimization history of the dissipated energy and natural frequency normalized to their initial values for both cases. Although the natural frequency increases by 18% in the first case due to the removal of 7 actu-

Table 3. Optimization results; Case 2.

		Initial	Iteration 1 (all)	Iteration 2 (−3,6,9)	Iteration 3 (−4,5)	Iteration 4 (−7,8)
Elem. No.						
	1	0.565	0.470	0.319	0.261	0.001
	2	0.565	0.470	0.319	0.261	0.001
Actuator	3	0.000	*0.000*	—	—	—
Energy	4	0.033	0.133	*0.004*	—	—
(Nm)	5	0.033	0.133	*0.004*	—	—
	6	0.000	*0.000*	—	—	—
	7	0.174	0.113	0.059	—	—
	8	0.174	0.113	0.059	*0.470*	—
	9	0.000	*0.000*	—	*0.470*	—
Total energy (Nm)		1.54	1.19	0.76	0.62	0.001
ω_1(Hz)		26.03	28.31	30.24	31.00	34.84
Mass (kg)		10.08	10.09	10.01	10.06	9.91
Gain (V sec/m)						
$\times 10^3$		3.00	2.51	1.62	1.24	1.10
t_1 (mm)		1.00	1.51	1.68	1.80	1.37
t_2 (mm)		1.00	0.96	0.78	0.90	1.31
t_3 (mm)		1.00	0.65	0.52	0.50	0.50
t_4 (mm)		1.00	0.92	1.04	0.86	0.83

ators, a more significant increase of 34% (from 26.03 Hz to 34.84 Hz) is observed in the second case since it is included as an objective function and structural parameters are used in the optimization formulation. A dramatic improvement is observed in the energy dissipation objective function, J, for Case 2. While J is reduced by 56% in Case 1, it is reduced almost to zero in Case 2. This is due to the inclusion of structural parameters in the optimization formulation which allows a more efficient design to be found. The total CPU time for Case 1 is approximately 5 minutes, while Case 2 requires approximately 15 minutes using an IBM RS6000 workstation.

CONCLUDING REMARKS

A formal optimization procedure has been developed to address the optimum design of a control system and a structure, simultaneously, using continuous design variables and a multiobjective optimization technique. Piezoelectric actuators bonded to a box beam are used as active damping elements for the purpose of vibration suppression. The finite element method using box beam elements is used to construct a model of the structure and the actuators. The Min$\Sigma\beta$ approach is used to formulate the multiobjective optimization problem. An algorithm is presented which determines optimal actuator locations as well as the most efficient structural configuration to be controlled by the actuators. This algorithm is implemented on a 2-D flexible structure. Two optimization cases are presented to illustrate the effectiveness of this procedure. In Case 1, the objective is to reduce the energy dissipated by the actuators with constraints imposed on the energy in the system and the modal damping ratios. The actuator gain is used as a design variable. In Case 2, the energy dissipated is minimized and the fundamental natural frequency is maximized simultaneously. An additional constraint is imposed on the mass of the structure. Box beam thicknesses are also included as design variables. The following observations are made from this study:

1. Piezoelectric actuators were more efficient when both their placements and the design of the structure were included in the optimization formulation.
2. The optimization procedure developed yielded significant improvements from an initial design to the final design.
3. A reduced number of actuators was necessary to control the structure in both cases.
4. Case 2 yielded a more efficient design.

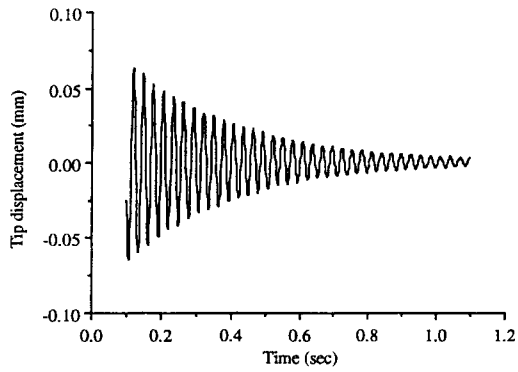

Figure 6. *Tip displacement final design case 2.*

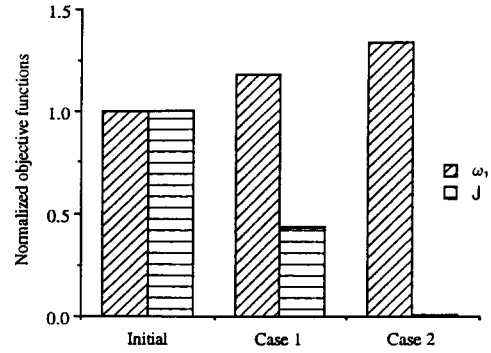

Figure 7. *Normalized natural frequency and dissipated energy case 2.*

REFERENCES

Banks, H. T., K. Ito and B. B. King. 1993. "Theoretical and Computational Aspects of Feedback in Structural Systems with Piezoceramic Controllers", *Center for Research in Scientific Computation Technical Report CRSC-TR93-2*, Raleigh, NC: North Carolina State University.

Banks, H. T., K. Ito and Y. Wang. 1992."Computational Methods for Identification and Feedback Control in Structures with Piezoceramic Actuators and Sensors", *Proc. Conference on Recent Advances in Adaptive and*

Sensory Materials and Their Applications, C. A. Rogers and R. C. Rogers, eds., Blacksburg, VA: Technomic Pub., VPI & SU, April 27–29, pp. 111–119.

Chattopadhyay, A. and T. McCarthy. 1991. "Multiobjective Design Optimization of Helicopter Rotor Blades with Multidisciplinary Couplings", *Structural Systems and Industrial Applications*, S. Hernandez and C. A. Brebbia, eds., pp. 451–461.

Crawley, E. F. and J. de Luis. 1987. "Use of Piezoelectric Actuators as Elements of Intelligent Structures", *AIAA Journal*, 25(10):1373–1385.

Dimitriadis, E. K., C. R. Fuller and C. A. Rogers. 1989. "Piezoelectric Actuators for Distributed Noise and Vibration Excitation of Thin Plates", *Proc. 8th ASME Conference on Failure, Prevention, Reliability and Stress Analysis*, Montreal, pp. 223–233.

Dosch, J., D. J. Inman and E. Garcia. 1992. "A Self-Sensing Piezoelectric Actuator for Collocated Control", *Journal of Intelligent Material System and Structures*, 3:166–185.

Fadel, G. M., M. F. Riley and J. F. Barthelemy. 1990. "Two Point Exponential Approximation Method for Structural Optimization", *Structural Optimization*, 2:117–124.

Gibbs, G. P. and C. R. Fuller. 1991. "Excitation of Thin Beams Using Asymmetric Piezoelectric Actuators", *Proc. 121st Meeting of the ASA*, Baltimore, MD, April, 1991.

Hanagud, S., M. W. Obal and A. J. Calise. 1992. "Optimal Vibration Control by the Use of Piezoceramic Sensors and Actuators," *Journal of Guidance, Control, and Dynamics*, 15(5):1199–1205.

Heeg, J. 1991. "An Analytical and Experimental Study to Investigate Flutter Suppression via Piezoelectric Actuation", Master's Thesis, George Washington University.

Horner, G. and J. Walz. 1985. "A Design Methodology for Determining Actuator Gains in Spacecraft Vibration Control", *Proc. 26th AIAA/ASME/ASCE/ASC Structures, Structural Dynamics and Materials Conference*, Orlando, FL, April 15–17, 1985, pp. 143–151.

Onoda, J. and Y. Hanawa. 1992. "Optimal Locations of Actuators for Statistical Static Shape Control of Large Space Structures: A Comparison of Approaches", *Proc. 31st AIAA/ASME/ASCE/AHS/ASC Structures, Structural Dynamics and Materials Conference*, Washington, DC: April 13–15, 1992, pp. 2788–2795.

1993. Piezo Systems Inc., *Product Catalog*.

Sepulveda, A. E., I. M. Jin and L. A. Schmit, Jr. 1992. "Optimal Placement of Active Elements in Control Augmented Structural Synthesis", *Proc. 31st AIAA/ASME/ASCE/AHS/ASC Structures, Structural Dynamics and Materials Conference*, Washington, DC: April 13–15, 1992, 2768–2787.

Vanderplaats, G. N. 1973. "CONMIN—A FORTRAN Program for Constrained Function Minimization", User's Manual, NASA TMX-62,282.